2011 50th IEEE Conference on Decision and Control and
European Control Conference (CDC-ECC)
Orlando, FL, USA, December 12-15, 2011

Nonstationary analysis of cerebral hemodynamics using recursively estimated multiple-input nonlinear models

Marios M. Markou, Marc J. Poulin and Georgios D. Mitsis

Abstract— **We present a computational scheme to obtain adaptive non-linear, multiple-input models of the Volterra-Wiener class, by utilizing Laguerre expansions of Volterra kernels in a recursive least-squares formulation. Function expansions have been proven successful in systems identification as they result in a significant reduction of the required free parameters, which is a major limiting factor particularly for nonlinear systems, whereby this number depends exponentially on the nonlinear system order. We apply this scheme in order to obtain adaptive estimates for a two-input model of cerebral hemodynamics, where the two inputs are arterial blood pressure (ABP) and end-tidal CO_2 (P_{ETCO_2}) variations and the output is cerebral blood flow velocity (CBFV) variations, by utilizing long-duration (40 min) experimental measurements of spontaneous variations of these signals in healthy humans. Maintenance of a relatively steady cerebral blood flow, despite changes in arterial pressure, is critical in order to meet the high metabolic demands of the brain. This is achieved by the synergistic action of various physiological factors, which may vary over different time-scales and also exhibit nonstationarities. We quantify these nonstationarities for the two main physiological determinants of cerebral blood flow variability (i.e., arterial pressure and arterial CO_2) by considering one- (ABP) and two-input (ABP and P_{ETCO_2}) models. The results illustrate the presence of nonstationarities which are frequency-dependent and also that incorporation of P_{ETCO_2} as an additional input, results in estimates of dynamic pressure autoregulation that are more consistent with respect to time.**

Index Terms: Cerebral autoregulation, recursive estimation, nonlinear modeling, nonstationary systems, Volterra models.

I. INTRODUCTION

Autoregulation of cerebral blood flow (CBF) is defined as the ability of the brain to maintain adequate blood flow despite variations in a number of external physiological variables, the most important of which is arterial blood pressure (ABP). It is now well established that autoregulation is a dynamic, frequency-dependent phenomenon [1], [2], [3], [4]. The reliable quantitative assessment of cerebral autoregulation and, more generally hemodynamics, is important in the context of cerebrovascular disease diagnosis [5]. This assessment may be performed by using spontaneous physiological variabilty, which exhibits broadband characteristics in the frequency range of interest, as well as step-like experimental ABP stimuli. Hemodynamics during resting conditions have been studied using both linear and nonlinear models, as well as one-input and multiple-input models ([1], [2], [4] among others). An important aspect of the obtained models is their time-varying characteristics, which are present in most physiological systems, due to their complexity and the consequent effect of several unobservable physiological variables and/or physiological cycles that act in widely different time scales (e.g., local mechanisms may act within seconds, whereas diurnal or circadian mechanisms have a cycle on the order of several hours). In the present paper, we propose a recursive scheme to estimate multiple-input Volterra models, which is based on Laguerre function expansions of Volterra kernels, and apply it in order to obtain adaptive two-input models of cerebral hemodynamics and examine the nonstationary characteristics of the cerebrovascular system. In order to do so, we utilize long duration experimental measurements of ABP, CBF and end-tidal CO_2 (P_{ETCO_2}) obtained under resting (spontaneous) conditions. We also examine the effect of unobservable physiological variables by comparing one-input (ABP) and two-input (ABP and P_{ETCO_2}) models. Our results extend the results of previous studies regarding nonstationarity of cerebral hemodynamics, based on wavelets and the autoregulatory index ([6], [7], [8]).

M.M. Markou and G.D. Mitsis are with the Department of Electrical and Computer Engineering, University of Cyprus, Nicosia 1678, Cyprus (e-mails: mmarkou@ucy.ac.cy, gmitsis@ucy.ac.cy)

M.J. Poulin is with the Departments of Physiology & Pharmacology and Clinical Neurosciences, Faculty of Medicine and Faculty of Kinesiology, University of Calgary, Canada (e-mail: poulin@ucalgary.ca)

II. METHODS

A. Experimental Methods

The experimental data were obtained at the University of Calgary from thirteen healthy subjects (age:29.1$\pm$4.8 years[mean$\pm$SD]) under normal, free-breathing conditions. None of the participants was on any medication and all of them were normotensive and did not have history of any cardiovascular, pulmonary or cerebrovascular diseases. ABP and CBFV were measured by finger photoplethysmography and transcranial Doppler ultrasonography in the right middle cerebral artery respectively, while P_{ETCO_2} was measured by mass spectrometry. The surrogate Doppler signal for CBF is the mean value of the velocity corresponding to the maximum Doppler shift $\hat{V_p}$ averaged over the entire cardiac cycle. Although it does not account for changes in vessel diameter, changes in $\hat{V_p}$ have been found to accurately reflect CBF changes in almost all practical cases, including resting conditions [9]. All experimental variables were sampled every 10 ms and beat-to-beat values of mean ABP (MABP) and mean CBF velocity (MCBFV) were calculated by integrating the waveform of the sampled signals within each cardiac cycle. The beat-to-beat values, as well as the breath-to-breath P_{ETCO_2} data were then interpolated and resampled at 1Hz to obtain equally spaced time series.

978-1-61284-799-3/11/$26.00 ©2011 IEEE

B. Mathematical Methods

1) Laguerre expansion of Volterra Kernels: The output of a non-linear multiple input single output system can be expressed in terms of a series of functionals [10] that represent higher order convolutions with the inputs signals:

$$\begin{aligned} y(n) = &\sum_{q=0}^{Q} \sum_{i_1=1}^{I} \cdots \sum_{i_q=1}^{I} \sum_{m_1} \cdots \sum_{m_q} k_q^{(x_{i_1} \ldots x_{i_q})}(m_1, \ldots, m_q) \times \\ &x_{i_1}(n-m_1) \ldots x_{i_q}(n-m_q) \\ = &\, k_0 + \sum_{i=1}^{I} \sum_{m} k_1^{(x_i)}(m) x_i(n-m) \\ + &\sum_{i_1=1}^{I} \sum_{i_2=1}^{I} \sum_{m_1} \sum_{m_2} k_2^{(x_{i_1} x_{i_2})}(m_1, m_2) \times \\ &x_{i1}(n-m_1) x_{i2}(n-m_2) + \ldots \end{aligned} \tag{1}$$

where I is the number of inputs. In the present case, $I = 2$ and the system inputs x_i are MABP and P_{ETCO_2}, while the system output $y(n)$ is MCBFV. k_q denotes the q-th order Volterra kernel of the system. The Volterra kernels describe the linear ($q = 1$) and nonlinear ($q > 1$) dynamic effects of the inputs (and their interactions) on the output. The sum of eq. (1) can be viewed as a generalization of the convolution sum, with the Volterra kernels quantifying the effect of past input values (linear kernel), as well as their q-th order products (nonlinear self- and cross-kernels) on the output at present time n. For causal and finite memory systems the sums in 1 are defined for $m_i = 0$ to M, where M is the system memory. In order to estimate the Volterra kernels using input-output measurements, we use the discrete Laguerre expansion method [11] formulated in a recursive least-squares context in order to continuously update our model estimates, as detailed below. This method utilizes the orthonormal Laguerre basis and requires the determination of two parameters: L and α where L is the maximum function order and α $(0 < \alpha < 1)$ determines the rate of exponential decay of the Laguerre functions - larger values of α result in slower decay and are thus more suitable for systems with large memory and/or slow dynamics. Determination of these parameters is discussed below. Using the Laguerre expansion method, the kernels can be expressed in the form:

$$\begin{aligned} k_1^{(x_i)}(m) &= \sum_{j_i=0}^{L_{x_i}} c_j^{(x_i)} b_j^{(x_i)}(m) \qquad i = 1, 2 \\ k_2^{(x_{i_1} x_{i_2})}(m_1, m_2) &= \sum_{j_1=0}^{L_{x_{i_1}}} \sum_{j_2=0}^{L_{x_{i_2}}} c_{j_1 \ldots j_q}^{(x_{i_1} \ldots x_{i_q})} b_{j_1}^{(x_{i_1})}(m_1) b_{j_2}^{(x_{i_2})}(m_2) \end{aligned} \tag{2}$$

where $i_1, i_2 = 1, 2$ and $b_j^{(x_i)}(m)$ is the j-th order discrete-time Laguerre function corresponding to input i, given by:

$$b_j^{(x_i)}(m) = \alpha_i^{(m-j)/2} (1-\alpha_i)^{1/2} \sum_{k=0}^{j} (-1)^k \binom{m}{k} \binom{j}{k} \alpha_i^{j-k} (1-\alpha_i)^k \tag{3}$$

By combining equations (1) and (2) we can write:

$$\mathbf{y} = \mathbf{V}\mathbf{c} + \epsilon, \tag{4}$$

where $\mathbf{y}$ is the $(N \times 1)$ vector of output observations, $\mathbf{V}$ is a $(N \times d)$ matrix containing the convolution of both inputs with the Laguerre functions $v_j^{(x_i)} = x_i * b_j^{(x_i)}$ (linear models), as well as higher-order products between them $v_{j_1}^{(x_{i1})} v_{j_2}^{(x_{i2})} \ldots v_{j_Q}^{(x_{iQ})}$ (nonlinear models), including self- and cross-terms (whereby $i_1 = i_2 = \cdots = i_Q$ and some of $i_1, i_2, \ldots, i_Q$ are different respectively), and $\mathbf{c}$ is the $(d \times 1)$ vector of the unknown expansion coefficients. The number of free parameters d is equal to $L + 1$ for $Q = 1$ and $L_1 L_2 + (L + L(L+1))/2$ for $Q = 2$,where $L = L_1 + L_2$, due to the symmetry of the second-order self-kernels with respect to $j_1, j_2, \ldots, j_Q$.

The values of $v_j^{(x_i)}$ can be obtained by the following recursive relations [12]:

$$v_j^{(x_i)}(n) = \sqrt{\alpha_i}(v_j^{(x_i)}(n-1) + v_{j-1}^{(x_i)}(n)) - v_{j-1}^{(x_i)}(n-1) \tag{5}$$

$$v_0^{(x_i)}(n) = \sqrt{\alpha_i} v_0^{(x_i)}(n-1) + \sqrt{1-\alpha_i} x_i(n) \tag{6}$$

The least-squares estimate of $\mathbf{c}$ is given by:

$$\hat{\mathbf{c}}_{LS} = (\mathbf{V}^T \mathbf{V})^{-1} \mathbf{V}^T \mathbf{y}. \tag{7}$$

2) Recursive estimation of the Laguerre expansion model: In order to obtain adaptive estimates for the system dynamics (self-kernels for MABP and P_{ETCO_2}, as well as cross-kernels between them) we formulate eq. (7) using recursive least squares. Initially, we rewrite the least-squares cost function at time point n as [13]:

$$J(n) = \sum_{s=1}^{N} \lambda^{n-s} e^2(s) \tag{8}$$

where $e(s)$ are the residuals at time point s and λ is the forgetting factor $(0 < \lambda \leq 1)$, which determines the weight of the previous time points on the present estimates. A smaller value of λ corresponds to models that adapt more quickly, while larger values of λ yield results that are closer to regular least-squares. The update equations for the coefficient vectors at time point n are then written as:

$$\hat{\mathbf{c}}(n) = \hat{\mathbf{c}}(n-1) + \mathbf{K}(n)\epsilon(n) \quad (9)$$

$$\epsilon(n) = y(n) - \mathbf{v}^T(n)\hat{\mathbf{c}}(n-1) \quad (10)$$

$$\mathbf{P}(n) = \frac{1}{\lambda}\left[\mathbf{P}(n-1) - \frac{\mathbf{P}(n-1)\mathbf{v}(n)\mathbf{v}^T(n)\mathbf{P}(n-1)}{\lambda + \mathbf{v}(n)^T\mathbf{P}(n-1)\mathbf{v}(n)}\right] \quad (11)$$

$$\mathbf{K}(n) = \frac{\mathbf{P}(n-1)\mathbf{v}(n)}{\lambda + \mathbf{v}^T(n)\mathbf{P}(n-1)\mathbf{v}(n)} \quad (12)$$

where $\mathbf{v}(n)$ is the n-th row of the matrix $\mathbf{V}$, $\mathbf{K}(n)$ is a gain matrix that determines the update size for $\hat{\mathbf{c}}(n)$ and $\mathbf{P}(n)$ is the estimate of the coefficient covariance matrix. The initial value for this matrix is typically selected as $\mathbf{P}(0) = \rho\mathbf{I}$. The effect of the value of λ on the results is examined below.

3) Model order selection: In order to select the model complexity (i.e., the value of L_{x_i} for each input), we utilized the Bayesian information criterion (BIC), which determines the optimal model structure as the one that minimizes:

$$BIC = \left(2 * \log\left[\frac{\sum_1^N (e(n))^2}{N-d-1}\right]\right) + (d * \log(N)) \quad (13)$$

where $e(n)$ are the residuals between the output measurements and the model output prediction and d,N were defined above as the number of model free parameters and number of observations respectively. Since the recursive estimation above (eqs. (9)-(12)) requires the use of a fixed structure for $\mathbf{V}$ we followed the following procedure for determining α_i and L_{x_i}: First, we segmented the entire 40 min data sets using sliding windows with a length of 300 sec (5 min) with a 1 min overlap. For each of the sliding windows we used regular least squares to select the optimal value of α_i as the value that minimized the normalized mean square error of the model prediction for a range of L_{x_i} values between 1 and 8. Consequently, for these optimal α_i values we selected the values of L_{x_i} (for $i = 1, 2$) which minimized the BIC criterion. For the recursive scheme, we used the median model order that resulted from this procedure, as the most representative for the entire data set.

C. Quantification of nonstationarities

The time varying characteristics of our model estimates were assessed in the frequency domain by using the following variability index:

$$I^{(x_i)}(f_i) = \frac{\left[\frac{1}{N_{\text{est}}-1}\sum_{j=1}^{N_{\text{est}}}(p_j^{(x_i)}(f_i) - \bar{p}^{(x_i)}(f_i))^2\right]}{\bar{p}^{(x_i)}(f_i)} \quad (14)$$

where $p_j^{(x_i)}(f_i)$ denotes the FFT magnitude of the first-order kernel corresponding to input x_i for the j-th data segment at frequency f_i, N_{est} is the total number of estimated kernels (we discarded the initial segments) and $\bar{p}(f_i)$ is the average of $p_j(f_i)$ over j at each frequency f_i.

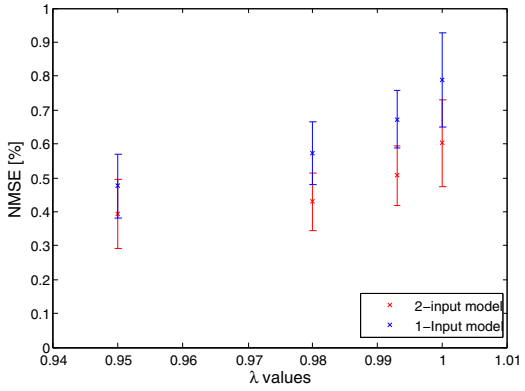

Fig. 1. Normalized Mean Square Error (NMSE) for one and two-input models as a function of λ (mean $\pm$ SD over all subjects).

III. RESULTS

The mean values of the MABP, P_{ETCO_2} and MCBFV measurements, averaged over the 40-min recordings for the thirteen subjects, were equal to 77.62 ± 5.54 mm Hg, 36.9 ± 3.77 mm Hg and 53.36 ± 4.63 cm/s respectively. In the following sections, we show results obtained for linear models (i.e., $Q = 1$ in eq. ((1)) both for one- and two-input models.

A. Effect of λ

As mentioned above, the forgetting factor λ, which lies in the range $(0,\ 1]$, determines the adaptive properties of the estimator. A value of unity is equivalent to regular least-squares, and indicates that all previous input values are equally significant in calculating the error function. As the value of λ reduces, the effective memory of the estimation algorithm reduces as well, and the estimates are affected relatively more by the immediately preceding input values. Therefore, smaller values of λ are more suitable for systems that are rapidly varying and/or have small memory, whereas larger values are suitable for slowly varying systems and systems with large memory.

We examine next the effect of λ on the variability index estimates. In Fig. (2) we show the variability index (eq. (14)) as a function of frequency for both the MABP (top panel) and P_{ETCO_2} (bottom panel) linear kernels. Note that in the case of linear models the first-order kernels are equivalent to the system impulse response; however, this does not hold for nonlinear models as the impulse response of the latter depends on the diagonal terms of the higher order kernels as well. It can be observed that the model estimates obtained with smaller λ values exhibit higher index values, i.e, higher variabililty, for both inputs. Also, the P_{ETCO_2} kernels are considerably more time-varying than their MABP counterparts, while the variability index is clearly frequency dependent, with the highest values being observed in the lowest frequencies.

B. Two-input models

In this section we present the results obtained from two-input models, i.e. when both MABP and P_{ETCO_2} were

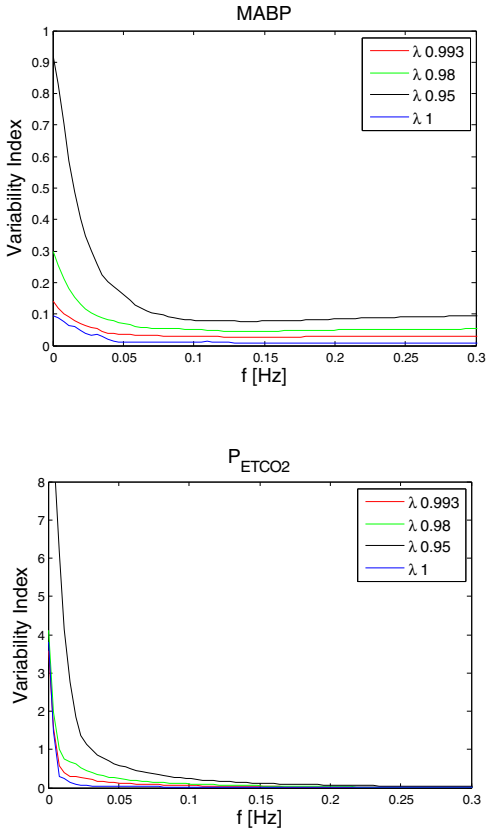

Fig. 2. Variability index (eq. (14)) for the linear MABP (top panel) and P_{ETCO_2} (bottom panel) kernels, averaged over all subjects, for two-input models and for various values of λ. Small values of λ result in estimates that exhibit strongly time-varying characteristics.

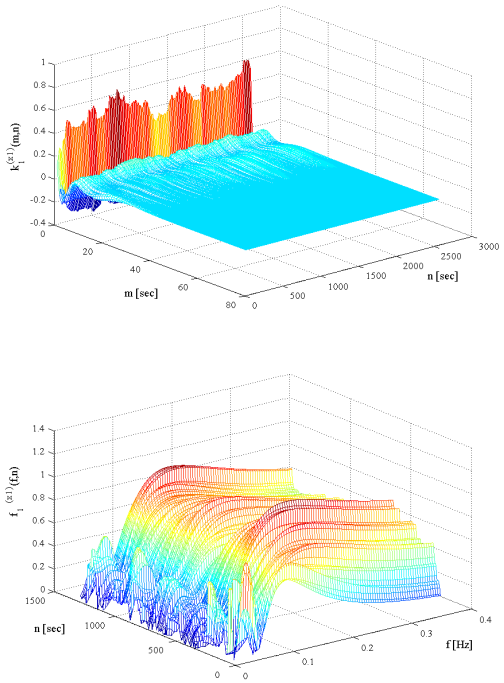

Fig. 3. Adaptive linear MABP kernels ($k_1^{(x_1)}$ in eq. (1)) estimates for one representative subject in the time (top panel) and frequency (bottom panel) domains as a function of time.

considered as input variables. The top panels of Figs. (3) and (4) illustrate the adaptive MABP and P_{ETCO_2} linear kernels in the time domain for one representative subject for $\lambda = 0.993$. We present results for this value, as it is adequate to capture the longer time scales present in dynamic autoregulation (previous studies have used 5-6 min segments to assess autoregulation from spontaneous measurements, e.g. [1], [4]). The MABP and P_{ETCO_2} linear kernels as well as the corresponding frequency responses are updated at each time point (i.e., every sec). The results in the frequency domain (bottom panels of Figs. (3) - (4)) illustrate the previously established high-pass characteristic for the MABP system dynamics, which implies more effective autoregulation of pressure variations below 0.15 Hz, and low-pass characteristic for the P_{ETCO_2} dynamics. The variability indices for the MABP and P_{ETCO_2} kernels, averaged over all subjects (mean $\pm$ standard deviation (SD)), are shown in Fig. (5), where it can be seen that the P_{ETCO_2} estimates are considerably more time-varying than their MABP counterparts. The MABP kernels are nonstationary mainly in the very low frequency range (below 0.04 Hz), while their characteristics for higher frequencies are relatively consistent. Also, note that the FFT magnitude values of the P_{ETCO_2} kernels above approximately 0.12 Hz is zero, as the corresponding input (end-tidal CO_2) is measured every breath (i.e. every 3-4 sec); therefore its power above 0.12 Hz is virtually zero.

C. Comparison between one-input and two-input models

Here we consider the effect of the second input (P_{ETCO_2}) on the time-varying characteristics of the MABP system dynamics, which reflect dynamic pressure autoregulation. This is done by considering one-input models, whereby the only input variable is MABP and the output is MCBFV and comparing the results to the two-input case considered above. In this case, the model of eq. (1) reduces to a one-input Volterra model, whereby the linear and nonlinear effects of MABP on MCBFV are described by the corresponding linear and nonlinear Volterra MABP kernels. As P_{ETCO_2} has a significant effect on MCBFV in the very-low and low-frequency ranges (mainly below 0.04 Hz [4]), we hypothesized that omission of P_{ETCO_2} would mainly affect the pressure autoregulation dynamics in these frequencies. The MABP dynamics obtained from a one-input model in the linear case are shown in Fig. (6) in the time domain (top panel) for one representative subject. Compared to the two input case (Fig. (4)), the obtained estimates exhibit a more pronounced slow component, consistent with our hypothesis. We also show the variability indices obtained from one and two-input models for the same subject in the bottom panel of Fig. (6), which illustrates that the variability index values are higher for one-input models. Finally, we show the variability index values for the MABP kernels averaged over

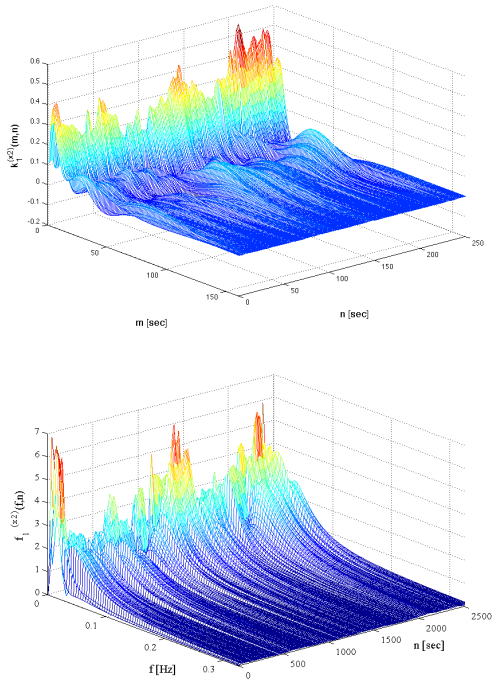

Fig. 4. Adaptive linear P_{ETCO_2} kernels ($k_1^{(x_2)}$ in eq. (1)) for the subject of fig. (3) in the time (top panel) and frequency (bottom panel) domains as a function of time.

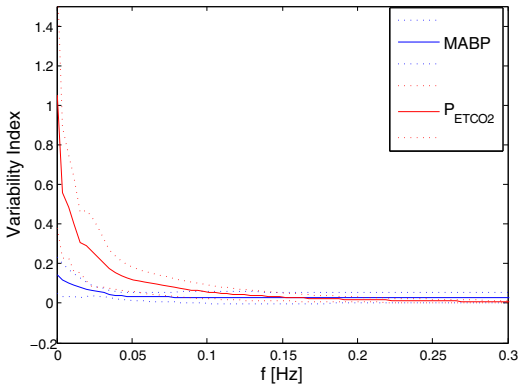

Fig. 5. Variability index for the linear MABP (blue) and P_{ETCO_2} (red) kernels, averaged over all subjects (mean±SD), as a function of frequency for $\lambda = 0.993$.

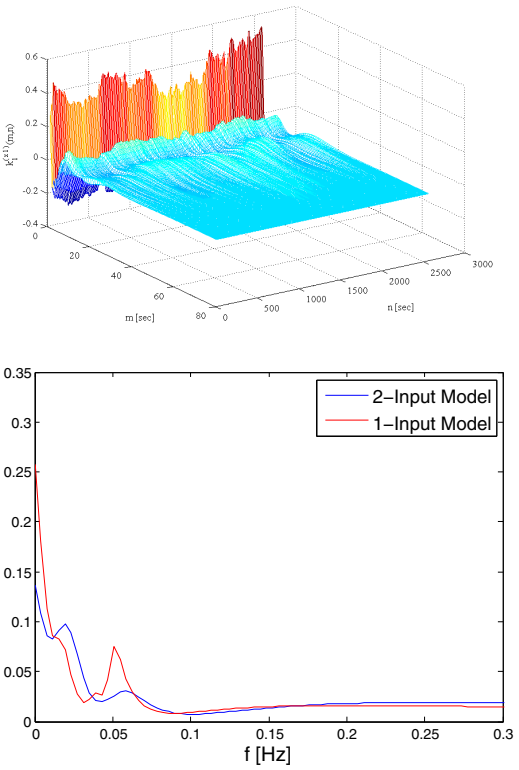

Fig. 6. Adaptive linear MABP kernels as a function of time obtained from one-input models for the subject of figs. (3)-(4) (top panel) and corresponding variability indices as a function of frequency for one-input and two-input models (bottom panel). Note that the one-input model results in higher variability index values overall.

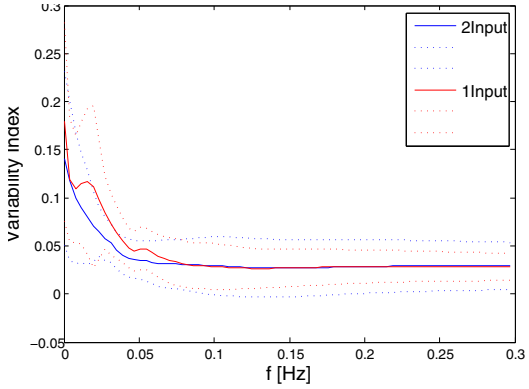

Fig. 7. Variability index comparison for linear MABP kernels, averaged over all subjects (mean ± SD) for one-input (red) and two-input(blue) models. One-input models result in higher variability values in the very low frequency range, due to the unmodeled effects of P_{ETCO_2}.

all subjects, as obtained from one- and two-input models in Fig. (7). The computed values are lower for two-input models over the entire frequency range, but the difference is more pronounced between 0.02 and 0.05 Hz, which is again consistent with our hypothesis and the results of Fig. (6).

IV. DISCUSSION

We have presented a recursive scheme for estimating nonlinear, multiple-input models, based on Laguerre expansions of Volterra kernels and applied this to obtaining adaptive models of cerebral hemodynamics. One of the main issues in nonlinear systems identification is the number of the required free parameters. In case of a Q-th order system with memory M, the number of free parameters in the standard least-squares formulation of the Volterra model is equal to M^Q. Utilizing function expansions reduces this number to L^Q, with the difference being more pronounced for nonlinear systems, since typically $L << M$. The recursive algorithm requires a fixed model structure; in order to determine

the most representative structure we utilized the BIC for overlapping 5 min segments using regular least-squares.

Obtaining accurate estimates of nonstationarities in physiological systems is particularly important, as these systems exhibit a high degree of complexity and are affected by many physiological factors that exert their effects over time scales that may be widely different. Therefore, in real-time applications it is important to track these nonstationarities in a reliable manner. In this context, selection of the parameter λ is important as it determines the adaptive properties of the estimation algorithm. This is shown in our results, as small λ values (e.g., 0.95) resulted in very variable estimates and also prediction errors that were very similar between one and two-input models. This is due to the fact that for this value of λ the effective memory of the estimation is small (for example $0.95^{20} = 0.36$), which implies that a small number of points affect the current estimates. This memory is rather short in order to account for the effects of P_{ETCO2}, which exhibit slower dynamics; therefore, we selected a larger value of λ, which is able to account for these slower dynamics, while allowing for adaptive tracking of cerebral hemodynamics. As MABP changes are the most important determinant of MCBFV changes, autoregulation is usually assessed by considering these effects only. Our results suggest that P_{ETCO2} affects the time-varying characteristics of MABP-MCBFV dynamics as well, therefore they should be taken into account as well. Specifically, the comparison between one- and two-input models reveals that the omission of P_{ETCO2} results in pressure autoregulation estimates that exhibit more pronounced time-varying behavior. The examination of these effects in nonlinear models of cebebral hemodynamics is currently underway and will be reported in subsequent studies.

V. ACKNOWLEDGEMENT

The authors would like to thank Dr. Philip Ainslie of the University of British Columbia at Okanagan for assistance with data collection.

REFERENCES

[1] R. Zhang, J. H. Zuckerman, C. A. Giller, and B. D. Levine, "Transfer function analysis of dynamic cerebral autoregulation in humans," American Journal of Physiology - Heart and Circulatory Physiology, vol. 274, no. 1, pp. H233–H241, 1998.

[2] R. B. Panerai, S. L. Dawson, and J. F. Potter, "Linear and nonlinear analysis of human dynamic cerebral autoregulation," American Journal of Physiology - Heart and Circulatory Physiology, vol. 277, no. 3, pp. H1089–H1099, 1999.

[3] G. Mitsis and V. Marmarelis, "Modeling of nonlinear physiological systems with fast and slow dynamics. i. methodology," Annals of Biomedical Engineering, vol. 30, pp. 272–281, 2002.

[4] G. Mitsis, J. M. Poulin, A. P. Ainslie, A. R. Peter, and V. Z. Marmarelis, "Nonlinear modeling of the dynamic effects of arterial pressure and co2 variations on cerebral blood flow in healthy humans," Biomedical Engineering, IEEE Transactions on, vol. 51, no. 11, pp. 1932 –1943, 2004.

[5] R. Panerai, "Cerebral autoregulation: From models to clinical applications," Cardiovascular Engineering, vol. 8, pp. 42–59, 2008.

[6] R. Panerai, P. Eames, and J. F. Potter, "Variability of time-domain indices of dynamic cerebral autoregulation," Physiological Measurement, vol. 24, 2003.

[7] M. Latka, M. Turalska, M. Glaubic-Latka, W. Kolodziej, D. Latka, and B. J. West, "Phase dynamics in cerebral autoregulation," American Journal of Physiology - Heart and Circulatory Physiology, vol. 289, pp. H2272–H2279, 2005.

[8] T. Peng, A. Rowley, P. Ainslie, M. Poulin, and S. Payne, "Wavelet phase synchronization analysis of cerebral blood flow autoregulation," Biomedical Engineering, IEEE Transactions on, vol. 57, no. 4, pp. 960 – 968, April 2010.

[9] M. J. Poulin and P. A. Robbins, "Indexes of flow and cross-sectional area of the middle cerebral artery using doppler ultrasound during hypoxia and hypercapnia in humans," Stroke, vol. 27, no. 12, pp. 2244–2250, 1996.

[10] V. Marmarelis, Nonlinear Dynamic Modeling of Physiological Systems. Piscataway, NJ: Wiley-Interscience & IEEE Press, 2004.

[11] ——, "Identification of nonlinear biological systems using laguerre expansions of kernels," Annals of Biomedical Engineering, vol. 21, pp. 573–589, 1993.

[12] H. Ogura, "Estimation of wiener kernels of a nonlinear system and a fast algorithm using digital laguerre filters," in Proc. 15th NIBB Conference, Okazaki, Japan, 1985, pp. 14–62.

[13] L. Ljung, System identification: Theory for the user. Upper Saddle River, NJ: Prentice Hall, 1999.